Industrial Crops & Products 174 (2021) 114226

Contents lists available at ScienceDirect

Industrial Crops & Products

journal homepage: www.elsevier.com/locate/indcrop

Differences in the content, composition and structure of the lignins from rind and pith of papyrus (*Cyperus papyrus* L.) culms

Mario J. Rosado [a,1], Florian Bausch [b,1], Jorge Rencoret [a], Gisela Marques [a], Ana Gutiérrez [a], Thomas Rosenau [b], Antje Potthast [b,*], José C. del Río [a,*]

[a] Instituto de Recursos Naturales y Agrobiología de Sevilla, CSIC, Avenida de la Reina Mercedes, 10, 41012 Seville, Spain
[b] Institute of Chemistry of Renewable Resources, University of Natural Resources and Life Sciences Vienna (BOKU), Konrad-Lorenz-Straße 24, A-3430 Tulln, Austria

ARTICLE INFO

Keywords:
Lignin
Papyrus
p-Coumarates
Ferulates
Tricin
Inter-unit linkages

ABSTRACT

Papyrus (*Cyperus papyrus* L.) is a plant with high productivity rate that is considered an interesting raw material for obtaining biofuels and biomaterials. In the present work, the composition and structural features of the lignins present in the rind and pith of papyrus culms have been studied. The analyses revealed that the lignins from both parts of papyrus culms differed greatly not only in their contents but also in composition and structure. In the rind, the lignin represented up to 27.0% (dry-matter) and was composed mainly of G-units (H:G:S composition of 4:63:33), while the lignin in the pith (15.7% dry-matter) presented a slightly higher amount of S-units (H:G:S composition of 8:43:49). These lignins also presented considerable amounts of cinnamates (*p*-coumarates and ferulates) incorporated. The differences in composition influenced the content of the lignin inter-unit linkages. Thus, the rind lignin presented lower amounts of β–*O*–4′ ether linkages (77% of all identified linkages) and higher content of condensed structures, such as phenylcoumarans (15%), resinols (2%), dibenzodioxocins (3%), and spirodienones (2%), while the pith lignin contained more β–*O*–4′ ethers (85% of all identified linkages) and lower amounts of phenylcoumarans (11%), tetrahydrofurans (2%), and spirodienones (2%). Moreover, 2D NMR analyses revealed that the lignins from papyrus were highly acylated at the γ-OH (40% acylation in the rind, and 60% acylation in the pith). DFRC analyses proved that *p*-coumarates were the main acylating groups, and that they were predominantly acylating the S-lignin units. Finally, the analyses also showed the presence of important amounts of the flavanone tricin in the rind lignin and, at lower amounts, in the pith lignin.

1. Introduction

Papyrus (*Cyperus papyrus* L.) is a rhizomatous perennial plant from the Cyperaceae. The plant is native to the wetlands of central, eastern and southern Africa and can grow well in tropical and subtropical climates. Papyrus form monotypic floating stands consisting of plant culms surmounted by an umbel that serves as the main photosynthetic surface, and reach heights of up to 5 m above the ground (Mnaya et al., 2007; Jones et al., 2018).

Papyrus is a plant that grows throughout the year and has a C4 photosynthetic pathway, which makes it one of the most productive herbaceous plants (Jones, 2011). The advantage of papyrus over other high-productivity C4 plants is that it grows in wetlands where the hydrological status is less seasonally variable. As result, the canopy is continuously maintained and culms continually develop from the rhizome (Jones and Muthuri, 1997). The standing dry matter of culms and umbels can reach up to 86.9 t DM ha^{-1}, and the aerial net primary production (NPP) can reach up to 136.4 t DM ha^{-1} yr^{-1} (Jones et al., 2018). The high rates of aerial productivity of this plant highlight its enormous potential as a source of biomass for producing biofuels or biomaterials in the context of a lignocellulosic biorefinery.

Papyrus is used primarily for making fences, roofs and mats, although their use to produce paper, fiberboard and briquettes are also emerging (Muthuri et al., 1989). Historically, papyrus had been cultivated and used by Ancient Egyptians for the production of papyri, a type of paper made from strips of the culm pith (Nicholson and Shaw, 2000). Papyrus is a lignocellulosic material that can also be used to produce biomaterials and biofuels. For this purpose, detailed investigation of the

* Corresponding authors.
E-mail addresses: antje.potthast@boku.ac.at (A. Potthast), delrio@irnase.csic.es (J.C. del Río).
[1] These are co-first authors

https://doi.org/10.1016/j.indcrop.2021.114226
Received 28 May 2021; Received in revised form 20 October 2021; Accepted 25 October 2021
Available online 4 November 2021

Table 1
Contents of the main constituents (as percent dry-weight) of the rind and pith of papyrus culms.[a]

	Papyrus rind	Papyrus pith
Acetone extractives	4.1 ± 0.1	4.9 ± 0.4
Methanol extractives	14.4 ± 0.6	14.2 ± 0.6
Water-soluble extractives	4.9 ± 0.2	7.7 ± 0.5
Klason lignin[b]	24.2 ± 0.5	13.2 ± 0.3
Acid-soluble lignin	2.8 ± 0.1	2.5 ± 0.1
Hemicelluloses	21.7 ± 0.1	20.8 ± 1.4
Cellulose	18.4 ± 0.2	29.3 ± 0.7
Proteins	4.5 ± 0.1	2.4 ± 0.1
Ash	5.0 ± 0.1	5.0 ± 0.2

[a] Average of three replicates
[b] Corrected for ash and proteins

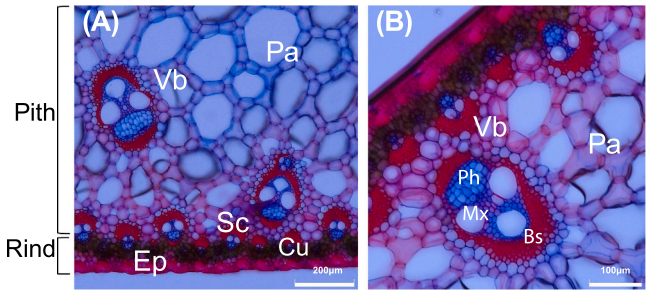

Fig. 1. Microscopic image of a cross-section of papyrus culm obtained with an Olympus DX 1000 digital microscope in incident light mode. (A) Detail of the anatomical parts of papyrus culm at 200 µm; Ep, epidermis; Cu, cuticle; Sc, schlerenchyma; Pa, parenchyma; Vb, vascular bundle. (B) Detail of a vascular bundle at 100 µm; Ph, phloem; Mx, metaxylem, Bs, bundle schlerenchyma. Lignin was stained red with Safranin-O, while the cellulosic parts were colored blue with Astra Blue. (For interpretation of the references to colour in this figure, the reader is referred to the web version of this article.)

Table 2
Weight-average (M_w) and number-average (M_n) molecular weights (g mol^{-1}), and polydispersity (M_w/M_n) of the MWLs from the rind and pith of papyrus culms.

	MWL rind	MWL pith
M_w	6000	6500
M_n	2920	3220
M_w/M_n	2.1	2.0

content and composition of their main components is essential. However, and despite the high number of studies regarding the cultivation of papyrus sedge as a potential source of biomass, studies on the detailed chemical composition of the plant components are comparatively scarce, and only one previous paper exists that reported the lignin composition in lignified cell walls of flowering stems of papyrus (Karlen et al., 2018).

It is now well recognized that lignin valorization is needed for a successful lignocellulosic biorefinery, including the emergence of 'lignin-first' methods that aim to preserve lignin for integrated or subsequent conversion to useful products (Rinaldi et al., 2016; Bajwa et al., 2019; Abu-Omar et al., 2021; Nguyen et al., 2021). Therefore, here we analyze the content, composition, and structure of the lignins located in the outer rind and the inner pith of the papyrus culm. The lignins will be analyzed "*in situ*" in the whole cell walls by analytical pyrolysis (Py-GC/MS) and Nuclear Magnetic Resonance (NMR) spectroscopy. For a more detailed analysis, the so-called "milled-wood lignin" (MWL) will be isolated from the rind and pith of papyrus culms using classical protocols, and will be analyzed by Py-GC/MS NMR, derivatization followed by reductive cleavage (DFRC) degradation method, and by Gel Permeation Chromatography (GPC). This study will provide important insights into the structure of these lignocellulosic materials that can be very useful for their subsequent valorization in a biorefinery.

2. Materials and methods

2.1. Samples and chemical analyses

Samples of papyrus (*Cyperus papyrus* L.) plant were collected from producers in Qaramos, Egypt. The plant samples were air-dried and the different parts of the culms (rind and pith) were separated manually. The dried samples were milled in an IKA cutting-mill to pass 1 mm screen.

The extractives contents of the rind and pith were measured by consecutive Soxhlet extraction with acetone (12 h), methanol (16 h) and hot water (12 h), and subsequent evaporation of the extracts in a rotovap. The Klason lignin and acid-soluble lignin contents were determined according to the TAPPI method T222 om-88 and the Tappi method UM 250, respectively (Tappi, 2004). Klason lignin content was corrected for ash and protein content (as indicated below for the whole samples). The holocellulose and α-cellulose contents were measured as previously described (Browning, 1967). The protein content was estimated from the N content determined in a LECO CHNS-932 Elemental Analyzer using a 6.25 factor (Darvill et al., 1980). The ash content was measured gravimetrically by incinerating the samples at 575 ºC for 6 h. Three replicates were used for each determination.

2.2. Microscopy analysis

For microscopy analysis, samples of papyrus culm tissue were impregnated with DP1500 polyethylene glycol, and were cut with a microtome. The transverse sections were stained with safranin-O and Astra blue. The samples were observed in incident light mode using an Olympus DX 1000 digital microscope.

2.3. Lignin isolation and purification

MWL preparations were isolated from the rind and pith of papyrus culms according to the standard protocol (Björkman, 1956). For this, around 100 g of pre-extracted rind and pith materials were ball-milled in a Retsch PM100 for a total of 16 h (in 20 min milling and 10 min resting intervals) using the conditions described previously (del Río et al., 2012a). The finely milled samples were extracted with dioxane-water (90:10, v/v) and purified as previously described (del Río et al., 2012a). The MWL yields represented ~10–15% of the total lignin content.

2.4. Gel Permeation Chromatography (GPC)

The MWLs were acetylated prior the GPC analyses. The samples were dissolved in tetrahydrofuran and the GPC analyses were performed on a Prominence-i LC-2030 3D GPC system equipped with a 300 mm × 7.5 mm i.d., 5 µm, PLgel MIXED-D column and a photodiode array (PDA) detector. The experimental conditions are published elsewhere (Rencoret et al., 2018).

2.5. Analytical pyrolysis

Pyrolysis of the whole rind and pith samples and their respective MWLs (~1 mg) was performed at 500 ºC (1 min), in the absence and in the presence of tetramethylammonium hydroxide (TMAH), in a 3030 micro-furnace pyrolyzer (Frontier Laboratories) connected to a GC 7820 A with an Agilent 5975 mass-selective detector. A capillary column DB-1701 (30 m × 0.25 mm i.d., 0.25 µm film thickness) was used, and the chromatographic conditions used for the analyses have been detailed elsewhere (del Río et al., 2012a). The identification of the carbohydrate

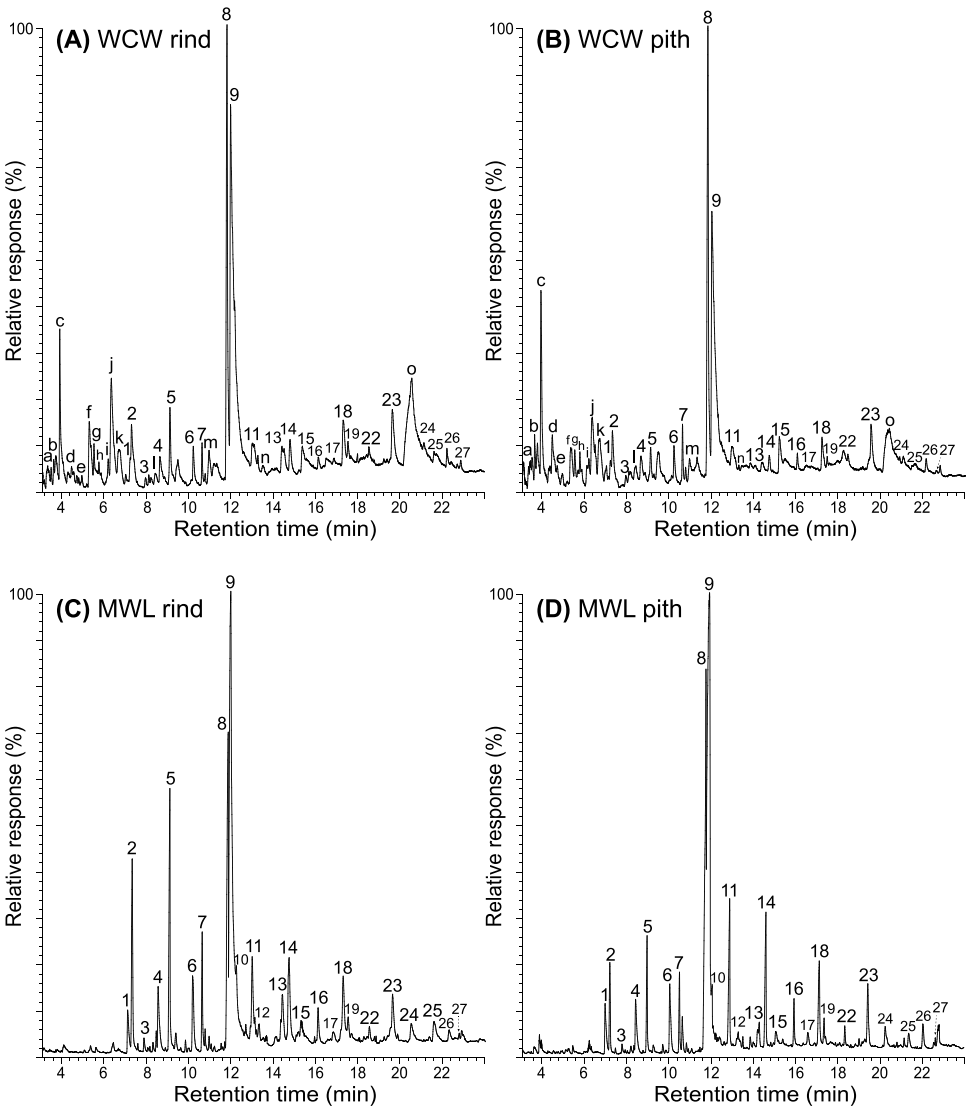

Fig. 2. Py-GC/MS of the whole cell walls (WCW) of papyrus rind (A), and papyrus pith (B), and of the MWLs from papyrus rind (**C**), and papyrus pith (D). The phenolic compounds released are listed in Table 3. Letters refer to carbohydrate-derived compounds: (a) (3*H*)-furan-2-one; (b) (2*H*)-furan-3-one; (c) furfural; (d) 2-hydroxymethylfuran; (e) cyclopenten-1-ene-3,4-dione; (f) 2,3-dihydro-5-methylfuran-2-one; (g) 5-methyl-2-furaldehyde; (h) 2-methyl-2-cyclopenten-1-one; (i) (5*H*)-furan-2-one; (j) 4-hydroxy-5,6-dihydro-(2*H*)-pyran-2-one; (k) 2-hydroxy-3-methyl-2-cyclopenten-1-one; (l) 3-hydroxy-2-methyl-(4*H*)-pyran-4-one; (m) 5-hydroxymethyl-2-tetrahydrofuraldehyde-3-one; (n) 5-hydroxymethyl-2-furaldehyde; (o) levoglucosan.

and lignin-derived compounds were accomplished by comparing their mass spectra with those reported in the literature (Ralph and Hatfield, 1991), and with our collection of standards. Data from two replicates were averaged and expressed as percentages.

2.6. 2D NMR spectroscopy

2D NMR were performed on a 500 MHz Bruker AVANCE III instrument equipped with a 5 mm TCI cryoprobe. The whole cell walls were analyzed at gel state as previously described (Kim et al., 2008; Rencoret et al., 2009). For this, around 70 mg of powdered rind and pith were swollen in 0.7 mL of DMSO-d_6 to form a gel. For the analysis of the MWLs, about 60 mg were dissolved in 0.6 mL of DMSO-d_6. HSQC and HMBC spectra were acquired using the Bruker's standard pulse programs "hsqcetgpsisp2.2″ and "hmbcgplpndqf", respectively, and using the experimental conditions published elsewhere (del Río et al., 2012b). The signals were assigned by literature comparison (Ralph et al., 2004a, 2004b; del Río et al., 2012a, 2012b, 2015). A semi-quantitative analysis of the signals in the HSQC spectra was performed using the Topspin 3.5 processing software from Bruker, as described elsewhere (del Río et al. 2012b). For the estimation of the H:G:S composition, it is important to take into account that the $C_{3,5}/H_{3,5}$ correlation signal of phenylalanine ($Phe_{3,5}$) in protein residues overlaps with the $C_{2,6}/H_{2,6}$ correlation signal of H-lignin units ($H_{2,6}$), overestimating its content (Kim et al., 2017). Therefore, the amounts of H-units were estimated by subtracting from the volume integral of the $H_{2,6}$ + $Phe_{3,5}$ signal the volume integral of the $Phe_{2,6}$ signal, a well-resolved signal that has a volume equivalent to that of $Phe_{3,5}$.

2.7. Derivatization followed by reductive cleavage (DFRC)

DFRC was carried out according to the original protocol (Lu and Ralph, 1997; Regner et al., 2018) and using the experimental conditions previously described (del Río et al., 2012a). DFRC degradation products were acetylated (Ac_2O/Py, 1:1) and then analyzed by GC-MS. The occurrence of native acetates was assessed by performing the DFRC using propionylating reagents, as previously published (Ralph and Lu, 1998; del Río et al., 2007a). The DFRC degradation products were analyzed by GC-MS using the conditions described elsewhere (del Río et al., 2012a, 2012b).

3. Results and discussion

3.1. Main constituents of the rind and pith of the papyrus culms

The contents of the main components present in the rind and pith of papyrus culms, namely acetone extractives, methanol extractives, water soluble extractives, lignin (Klason and acid-soluble lignins),

Table 3
Identities and relative molar abundances (%) of the phenolic compounds released upon Py-GC/MS of the whole cell walls (WCW) and MWLs from the rind and pith of papyrus culms.

Label	Compound	Origin	Papyrus Rind		Papyrus Pith	
			WCW	MWL	WCW	MWL
1	phenol	H	1.2	2.4	1.2	3.3
2	guaiacol	G	4.3	6.6	3.7	3.2
3	3-methylphenol	H	0.5	0.5	0.9	0.4
4	4-methylphenol	H	2.1	3.3	2.7	3.4
5	4-methylguaiacol	G	3.8	7.5	1.6	3.3
6	4-ethylphenol	H	1.5	2.4	2.0	3.6
7	4-ethylguaiacol	G	1.2	2.7	1.8	2.1
8	4-vinylguaiacol	G/FA	17.2	10.3	22.1	14.6
9	4-vinylphenol	H/*p*CA	50.9	43.2	47.7	45.4
10	eugenol	G	0.6	0.6	0.2	0.2
11	syringol	S	1.2	3.0	2.5	4.7
12	*cis*-isoeugenol	G	0.3	0.5	0.1	0.1
13	*trans*-isoeugenol	G	2.5	2.4	0.8	0.9
14	4-methylsyringol	S	1.6	2.3	1.0	3.8
15	vanillin	G	2.3	1.4	2.4	1.0
16	4-ethylsyringol	S	0.5	0.9	0.8	1.0
17	acetovanillone	G	0.4	0.7	0.2	0.6
18	4-vinylsyringol	S	2.2	2.6	2.0	2.9
19	4-allylsyringol	S	0.6	0.5	0.6	0.5
20	guaiacylacetone	G	0.2	0.2	0.1	0.3
21	propiovanillone	G	0.0	0.2	0.0	0.1
22	*cis*-4-propenylsyringol	S	0.4	0.5	0.6	0.4
23	*trans*-4-propenylsyringol	S	2.9	2.1	3.4	1.8
24	syringaldehyde	S	0.5	1.2	0.6	0.7
25	acetosyringone	S	0.5	1.4	0.2	0.6
26	syringylacetone	S	0.5	0.5	0.5	0.8
27	propiosyringone	S	0.1	0.1	0.2	0.1
		H* =	18.1	19.7	24.4	28.7
		G* =	52.3	51.6	38.7	32.5
		S* =	29.6	28.8	36.9	38.8
		S/G* =	0.57	0.56	0.95	1.20

* Estimated without using the abundances of 4-vinylguaiacol (**8**, arising also from ferulates), 4-vinylphenol (**9**, arising also from *p*-coumarates), and the analogous 4-vinylsyringol (**18**). H: *p*-hydroxyphenyl units; G: guaiacyl units; S: syringyl units; *p*CA: *p*-coumarates; FA: ferulates.

carbohydrates (hemicelluloses and cellulose), proteins, and ashes, are shown in Table 1. The rind and pith contained high amounts of extractives that amounted to 23.4% in the rind, and up to 26.8% in the pith (including the acetone, methanol and water-soluble extractives), methanol extractives being the most abundant (~ 14%) in both materials. The total lignin content (Klason + acid soluble) in the rind represented 27.0% of the dry material, while the lignin content in the pith was significantly lower, accounting for only 15.7% of the dry material. The rind and the pith had a similar content of hemicelluloses (21.7% in the rind, and 20.8 in the pith) but the cellulose content was much higher in the pith (29.3%) than in the rind (18.4%). Both materials also presented significant protein contents that accounted for 4.5% in the rind and 2.4% in the pith. Finally, the rind and the pith also contained some amount of ash, representing 5.0% in the rind and pith.

Microscopic study of histological sections of papyrus culms by microtome cutting was also carried out to gain more information on the distribution of lignin (Fig. 1). The microscopic image clearly corroborated that the lignin (red-stained) was more concentrated in the rind than in the pith, which is more enriched in cellulose (blue-stained), and in agreement with the data from the compositional analysis. The images showed that the lignin was mainly located in the sclerenchyma tissue of the culms, and strengthening the vascular bundles.

In this work, to study in detail the lignins of the rind and pith of papyrus culms, MWL preparations were isolated by aqueous dioxane extraction using the classical procedure (Björkman, 1956), which is highly recommended to obtain a lignin preparation with minimal structural alterations. MWLs were chemically characterized by GPC, which provided information on the molecular weights of both lignins, Py-GC/MS (in the absence and in the presence of TMAH), which afforded data on the composition of the lignin and *p*-hydroxycinnamates units, 2D NMR spectroscopy for information on both the lignin units (including *p*-hydroxycinnamates and tricin) and on different inter-unit linkages, and DFRC degradation, which allowed addressing the nature and extent of lignin side-chain acylation, as well as the different lignin monomers involved in β-ether linkages.

3.2. Molecular weight distribution of the lignins

The molecular weight-average (M_w) and number-average (M_n) values of the MWLs from the rind and pith of the papyrus culms were determined from the GPC curves, and the data are shown in Table 2. Both MWLs exhibited rather similar molecular weights, with a M_w comprised between 6000 and 6500 g/mol for the lignins of the rind and pith, respectively, and a M_n comprised between 2920 and 3220 g/mol for the lignins of the rind and pith, respectively. The MWLs exhibited relatively low polydispersity, with M_w/M_n around 2.0–2.1, compared to other lignins (Rencoret et al., 2018), which indicates that the lignins isolated from papyrus were quite homogeneous (Tolbert et al., 2014).

3.3. Lignin composition of the rind and pith as determined by Py-GC/MS

The lignins of the rind and pith of papyrus culms were analyzed using Py-GC/MS, a thermal degradation technique that provides rapid information on their constituent units. The lignins were analyzed both "*in situ*" in the whole cell walls (Fig. 2, top), as well as in their respective MWL preparations (Fig. 2, bottom). The whole cell walls released carbohydrate-derived compounds (labeled with letters from *a* to *o*), as well as phenolic compounds that are derived from lignin and from *p*-hydroxycinnamates. The pyrograms of the MWLs released only phenolic compounds that matched those released from the whole cell walls. The identities of the phenolic compounds released are listed in Table 3, together with their relative molar abundances.

The phenolic compounds released upon Py-GC/MS are derived from the three lignin units (*p*-hydroxyphenyl, H, guaiacyl, G, and syringyl, S). The most prominent phenolic compounds released from the whole rind and pith, as well as from the MWLs, were 4-vinylphenol (**9**), which accounted for nearly half of all released phenolic compounds, and 4-vinylguaiacol (**8**), which was especially abundant in the pyrograms of the whole cell walls of rind and pith. Other phenolic compounds were also released, although to a lesser extent, such as phenol (**1**), 4-methylphenol (**4**), 4-ethyphenol (**6**), guaiacol (**2**), 4-methylguaiacol (**5**), 4-ethylguaiacol (**7**), *trans*-isoeugenol (**13**), syringol (**11**), 4-methylsyringol (**14**), 4-ethylsyringol (**16**), 4-vinylsyringol (**18**), and *trans*-4-propenylsyringol (**23**), among others.

The extremely high abundance of 4-vinylguaiacol (**8**) and 4-vinylphenol (**9**) released from the papyrus lignins seems to indicate that these compounds do not arise entirely from lignin units but may also arise from ferulates and *p*-coumarates that are known to decarboxylate under pyrolytic conditions, as has been observed in the pyrolysis of other lignins (del Río et al., 1996, 2007b, 2012a, 2012b, 2015; Rencoret et al., 2015; Rosado et al., 2021). Interestingly, the relative abundance of 4-vinylguaiacol (**8**) was lower in the MWLs than in the respective whole cell walls, because most of it arises from ferulates that are mostly linked to carbohydrates, which are removed during the extraction of the MWL.

Theoretically, the H:G:S composition of the lignins of the rind and pith of the papyrus culms could be estimated by integrating the peak areas of the respective H-, G-, and S-lignin units. However, since most of 4-vinylguaiacol (**8**) and 4-vinylphenol (**9**) arise from *p*-hydroxycinnamates, it is clear that these phenolic compounds cannot be utilized to estimate the H:G:S composition from Py-GC/MS. However, an approximate estimation of the H:G:S compositions of these lignins could be obtained by using the peak areas of all H-, G- and S-derived compounds, except 4-vinylphenol (which is mostly produced from *p*-

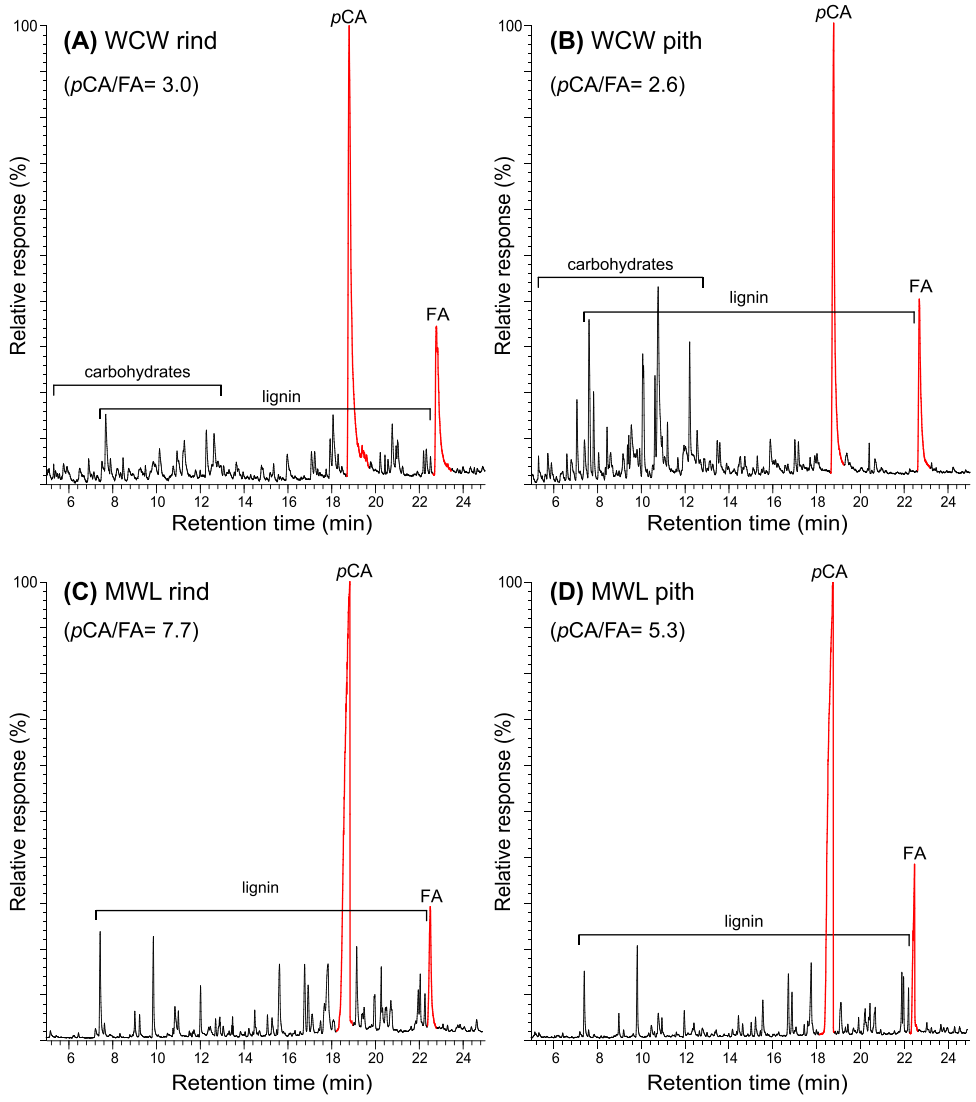

Fig. 3. Py-TMAH-GC/MS of the whole cell walls (WCW) of papyrus rind (A), and papyrus pith (B), and of the MWLs from papyrus rind (C), and papyrus pith (D). *p*CA and FA are the fully methylated *p*-coumaric and ferulic acids, respectively.

coumarates), 4-vinylguaiacol (that is mostly produced from ferulates), and the respective 4-vinylsyringol (**18**), as was previously done for other lignins with high contents of *p*-hydroxycinnamates (del Río et al., 2012a, 2012b, 2015, 2018; Rencoret et al., 2015; Rosado et al., 2021). The lignin composition estimated in this way indicated that the lignins of the rind and pith of papyrus culms were quite different: the lignin of the rind was enriched in G-lignin units (S/G 0.56), while the pith lignin presented a slight predominance of S-lignin units (S/G 1.20).

As stated above, *p*-coumaric and ferulic acids cannot be directly analyzed by analytical pyrolysis. However, the presence of *p*-hydroxycinnamic acids in these lignins were successfully assessed by accomplishing the pyrolysis in the presence of a methylating reagent, tetramethylammonium hydroxide (TMAH), that avoids decarboxylation by producing the methyl derivatives of the carboxylic groups as well as the phenols (del Río et al., 1996, 2007b), as shown in Fig. 3. Py-TMAH of the whole rind and pith of papyrus culms and of their respective MWLs released large amounts of the fully methylated *p*-coumaric (***p*CA**) and ferulic (**FA**) acids, confirming the high abundance of these *p*-hydroxycinnamic acids in the lignins of papyrus culms. Integration of the peak areas of *p*CA and FA in the Py-TMAH chromatograms showed that the content of FA was lower in the MWLs than in the respective whole cell walls, as can be seen in the *p*CA/FA ratios which increased from 3.0 to 7.7 in the rind, and from 2.6 to 5.3 in the pith. These data indicate that in papyrus FA is mainly linked to the carbohydrates, while *p*CA is mainly linked to the lignin, similar to what occurs in other plants, particularly in grasses (Ralph, 2010; Hatfield et al., 2017).

3.4. *Lignin composition and inter-unit linkages as determined by 2D NMR*

The whole cell walls and the MWL preparations were also analyzed by 2D NMR, which provided detailed data of lignin composition as well as of the different lignin inter-unit linkages. The HSQC spectra of the whole cell walls and the MWL preparations from the rind and pith of papyrus culms are shown in Fig. 4, together with the main lignin substructures found. The HSQC of the whole cell walls exhibited signals from both carbohydrates and lignin structures, while the HSQC of the MWLs primarily presented lignin signals which essentially matched those in the spectrum of the whole cell walls. This was particularly evident in the aromatic regions of the spectra where signals from carbohydrates do not appear, and indicated that the MWLs were rather representative of the native lignins in papyrus.

The side-chains regions of the HSQC provided information regarding the inter-unit linkages present in the lignin, which were seen more clearly in the spectra of the MWLs due to the absence of carbohydrates. Correlation signals of typical lignin substructures, such as β–*O*–4′ alkyl-aryl ethers (**A**), phenylcoumarans (**B**), resinols (**C**), dibenzodioxocins

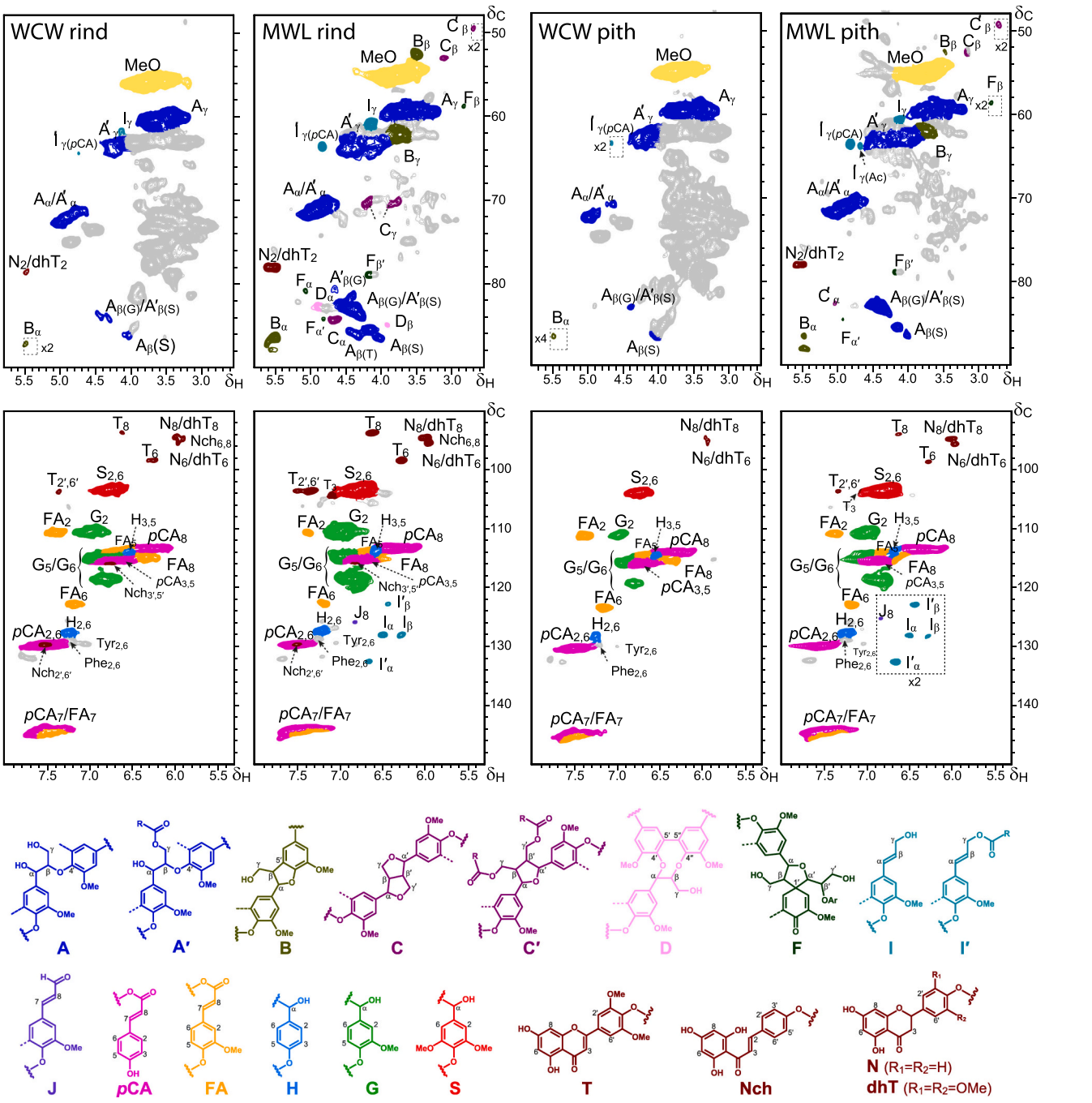

Fig. 4. Side-chain (δ_C/δ_H 48–90/2.5–5.8, top) and aromatic (δ_C/δ_H 90–150/5.3–8.0, bottom) regions of the HSQC spectra of the whole cell walls (WCW) and the MWLs from the rind and pith of papyrus culms. The lignin structures identified are shown below. A: β–*O*–4′ alkyl-aryl ethers; A′: γ-acylated β–*O*–4′ alkyl-aryl ethers; B: phenylcoumarans; C: resinols; C′: γ-acylated tetrahydrofurans; D: dibenzodioxocins; F: spirodienones; I: *p*-hydroxycinnamyl alcohol end-groups; I′: γ-acylated *p*-hydroxycinnamyl alcohol end-groups; J: *p*-hydroxycinnamaldehyde end-groups; *p*CA: *p*-coumarates; FA: ferulates; H: *p*-hydroxyphenyl units; G: guaiacyl units; S: syringyl units; T: tricin; Nch: naringenin chalcone; N: naringenin; dhT: dihydrotricin. Signals from protein residues of phenylalanine (Phe) and tyrosine (Tyr) are indicated.

(**D**), spirodienones (**F**), and *p*-hydroxycinnamyl alcohol end-groups (**I**), were clearly seen in this region. The spectra also showed strong signals corresponding to lignin structures acylated at the γ-OH of the side-chain, including signals of γ-acylated β–*O*–4′ alkyl-aryl ethers (**A′**), γ-acylated tetrahydrofurans (**C′**), and γ-acylated *p*-hydroxycinnamyl alcohol end-groups (**I′**). The degree of γ-acylation of the lignin side-chains was estimated from the C_γ/H_γ correlation signals in γ-OH (A_γ) and γ-acylated β–*O*–4′ alkyl-aryl ethers (A'_γ), and indicated that the papyrus lignins were highly acylated at the γ-OH, with a degree of acylation reaching up to 40% in the rind and 60% in the pith. Characteristic signals from *p*-hydroxycinnamyl alcohol end-groups acylated with *p*-coumarates (*p*CA) were observed in the HSQC of both lignins at δ_C/δ_H 63.9/3.13 ($I_{\gamma(pCA)}$) suggesting that *p*CA was the main group that acylated the γ-OH in these lignins. In addition, the HSQC of the MWL of the pith also showed a small signal at δ_C/δ_H 64.1/4.63 ($I_{\gamma(Ac)}$) which is characteristic of acylation with acetates, indicating that acetates also occur acylating the side-chain of this lignin, although to a lower extent. Lignin acylation with *p*CA is a characteristic of many plants, particularly grasses and other commelinid monocots (Karlen et al., 2018; del Río et al., 2012a, 2015; Ralph, 2010; Hatfield et al., 2017), whereas lignin acylation with

Table 4
Structural characteristics (inter-unit linkages, *p*-hydroxycinnamyl end-groups, degree of γ-acylation, H-, G-, and S-lignin units, S/G ratios, *p*-hydroxycinnamate, and tricin contents) from integration of the signals in the HSQC of the whole cell walls (WCW) and the MWLs from the rind and pith of papyrus culms.

	Papyrus rind		Papyrus pith	
	WCW	MWL	WCW	MWL
Lignin inter-unit linkages (%)				
β–*O*–4′ aryl ethers (**A**/**A′**)	–	77	–	85
β–5′ Phenylcoumarans (**B**)	–	15	–	11
β–β′ Resinols (**C**)	–	2	–	tr.
β–β′ Tetrahydrofurans (**C′**)	–	1	–	2
5–5′ Dibenzodioxocins (**D**)	–	3	–	0
β–1′ Spirodienones (**F**)	–	2	–	2
Lignin end-groups[a]				
Cinnamyl alcohol end-groups (**I**/**I′**)	–	8	–	12
Cinnamaldehyde end-groups (**J**)	–	3	–	2
Degree of γ-acylation (%)	–	40	–	60
Lignin aromatic units[b]				
H (%)	7	4	11	8
G (%)	61	63	45	43
S (%)	32	33	44	49
S/G ratio	0.52	0.52	0.98	1.14
p-Hydroxycinnamates[c]				
p-coumarates (***p*CA**)	77	49	95	84
ferulates (**FA**)	27	7	62	13
p-coumarates/ferulates ratio	2.85	7.00	1.53	6.46
Tricin (**T**)[c]	6	6	2	2

[a] Expressed as a fraction of the total lignin inter-unit linkage types **A**-**F**
[b] Molar percentages (H+G+S=100)
[c] *p*-Hydroxycinnamates and tricin contents referred as percentages of total lignin content (H+G+S)

acetates is widely distributed among the lignins in all angiosperms (Ralph, 1996; del Río et al., 2007a, 2008). It is interesting to note the appearance of signals of γ-acylated tetrahydrofurans (**C′**), although at a low level, which are produced from β–β′ coupling of previously acylated monolignols. After β − β′ coupling of two monolignols, the intermediate quinone methide rearomatizes by internal trapping of the γ-OH producing the resinol structure, however, in the case of γ-acylated monolignols internal trapping cannot occur and instead tetrahydrofuran structures will be produced. The occurrence of γ-acylated tetrahydrofurans in the papyrus lignins demonstrate that the lignin acylation occurred at monolignol level, and that the acylated monolignols act as authentic lignin monomers in these lignins participating in coupling reactions, as it has been previously demonstrated in other highly acylated lignins (Lu and Ralph, 2002, 2005, 2008; del Río et al., 2007a, 2008, 2015; Lu et al., 2015).

The aromatic/unsaturated regions of the HSQC spectra showed signals that corresponded mainly to the different lignin (H, G, S) and *p*-hydroxycinnamate (*p*CA, FA) units, along with some signals from protein residues. The correlation signals for the unsaturated bonds (C_α/H_α and C_β/H_β) of normal γ-OH (I_α, I_β) and γ-acylated (I'_α, I'_β) cinnamyl alcohol end-groups, as well as the C_8/H_8 correlation signal of cinnamaldehyde end-groups (I_8), also appeared in this region of the spectra. Signals from the flavone tricin were also present in the HSQC of both lignins, with the typical correlations signals for C_8/H_8 (T_8) and C_6/H_6 (T_6) at δ_C/δ_H 94.6/6.58 and 98.7/6.22 (del Río et al., 2012b), indicating that tricin is also incorporated into the papyrus lignins, as it also occurs in the lignins of grasses and in other monocots (del Río et al., 2012b, 2015, 2020, 2021; Rencoret et al., 2013; Lan et al., 2015, 2016). Interestingly, tricin was also found in the lignin of the related sedge *Carex heleonastes* (Pikovskoi et al., 2020). In addition to tricin, the HSQC of the lignins of the rind and pith of papyrus culms also showed other signals in the aromatic regions at δ_C/δ_H 95.8/5.91 and at δ_C/δ_H 94.8/5.93, that were assigned to the C_6/H_6 and C_8/H_8 correlations of the flavanones naringenin (N_6, N_8) and dihydrotricin (dhT_6, dhT_8), along with the $C_{6,8}/H_{6,8}$ correlations of naringenin chalcone ($Nch_{6,8}$) that was only present in the rind lignin (Rencoret et al., 2021). The signal for the C_2/H_2 correlations of the flavanones naringenin (N_2) and dihydrotricin (dhT_2) was also observed in the aliphatic regions of the spectra at δ_C/δ_H 78.5/5.44. Some flavanones, as eriodictyol and dihydrotricin, can cross-couple with monolignols to form flavanolignans, indicating their compatibility with lignification (Chang et al., 2010; Csupor et al., 2016; Yuan et al., 2019). The detailed identification of these flavonoids in the papyrus rind lignin, their mechanism of incorporation into the lignin polymer, and their potential biosynthetic pathway, have been published elsewhere (Rencoret et al., 2021).

The structural characteristics of the lignins of the rind and pith of papyrus culms, including the abundances of the different linkages and the *p*-hydroxycinnamyl end-groups, the degree of γ-acylation, the relative abundances of the H-, G- and S-lignin units, the S/G ratios, the *p*-hydroxycinnamate content, and the contents of tricin, estimated from the HSQC spectra, are shown in Table 4. The lignins of papyrus culms presented an H:G:S composition of 4:63:33 (S/G 0.52) for the rind, and 8:43:49 (S/G of 1.14) for the pith, which are in agreement with the data obtained upon Py-GC/MS. The NMR data also indicated the occurrence of important amounts of *p*-coumarates (49% and 84% in the rind and pith, respectively) along with lower amounts of ferulates (7% and 13% in the rind and pith, respectively). The NMR data indicated that the ferulate content was greatly reduced in the MWLs when compared to the whole cell walls. This was clearly reflected in the *p*CA/FA ratios of the whole cell walls (2.85 in the rind and 1.52 in the pith) which was greatly increased in the spectra of the MWLs (7.0 in the rind and 6.46 in the pith), indicating that ferulates, which were preferentially attached to carbohydrates, were selectively removed during the MWL isolation process, as already observed upon Py-TMAH. This corroborates that in papyrus, *p*-coumarates are linked to the lignin polymer, while ferulates are mainly bound to carbohydrates, as is also the case with grasses (del Río et al., 2015; Ralph, 2010). A previous work analyzed "*in situ*" the lignin of lignified cell walls of flowering stems of papyrus by 2D NMR, and reported an H:G:S composition of 9:39:61 (S/G 0.64), together with significant amounts of *p*-coumarates acylating the γ-OH of the lignin as well as ferulates attached to the cell wall (Karlen et al., 2018). The ferulate content in the papyrus lignins (7% in the rind, and 13% in the pith) seems to be among the highest values reported in lignins. For comparison, the FA content in other lignins, such as those from sugarcane bagasse and straw (4–5%), or rice husks and straw (4%), are much lower (del Río et al., 2015; Rosado et al., 2021). The lignins of the rind and pith of papyrus culms also contained significant amounts of the flavone tricin (T), which was more abundant in the rind where it accounted for 6%, referred to total lignin units, while in the pith it was only 2%.

Regarding the inter-unit linkages, the rind lignin, which is enriched in G-lignin units, had lower amounts of β–*O*–4′ alkyl aryl ether linkages (77% of all identified linkages) and higher amounts of phenylcoumarans (15%), together with minor amounts of other condensed linkages (resinols, 2%; tetrahydrofurans, 1%; dibenzodioxocins, 3%; and spirodienones, 2%), as well as *p*-hydroxycinnamyl alcohol end-groups (8%) and cinnamaldehydes (3%). The lignin from the pith, on the contrary, presented higher amounts of β–*O*–4′ alkyl aryl ether linkages (85% of all identified linkages), as corresponds to a lignin with a higher content of S-lignin units, as well as lower amounts of phenylcoumarans (11%), and minor amounts of other condensed linkages (tetrahydrofurans, 2%; spirodienones, 2%) and *p*-hydroxycinnamyl alcohol end-groups (12%) and *p*-hydroxycinnamaldehydes (2%). Dibenzodioxocins were not found in this lignin and only traces of resinols were detected.

The papyrus lignins presented extremely low amounts of resinol substructures, accounting for only 2% of all linkages in the rind lignin, whereas they were detected in trace amounts in the pith lignin. This seems to be related to the high degree of acylation of the γ-OH in these lignins, as was also observed in other highly acylated lignins (del Río et al., 2007a, 2008, 2012a, 2015). As said above, β–β′ coupling of γ-acylated monolignols cannot form resinol structures, but will form

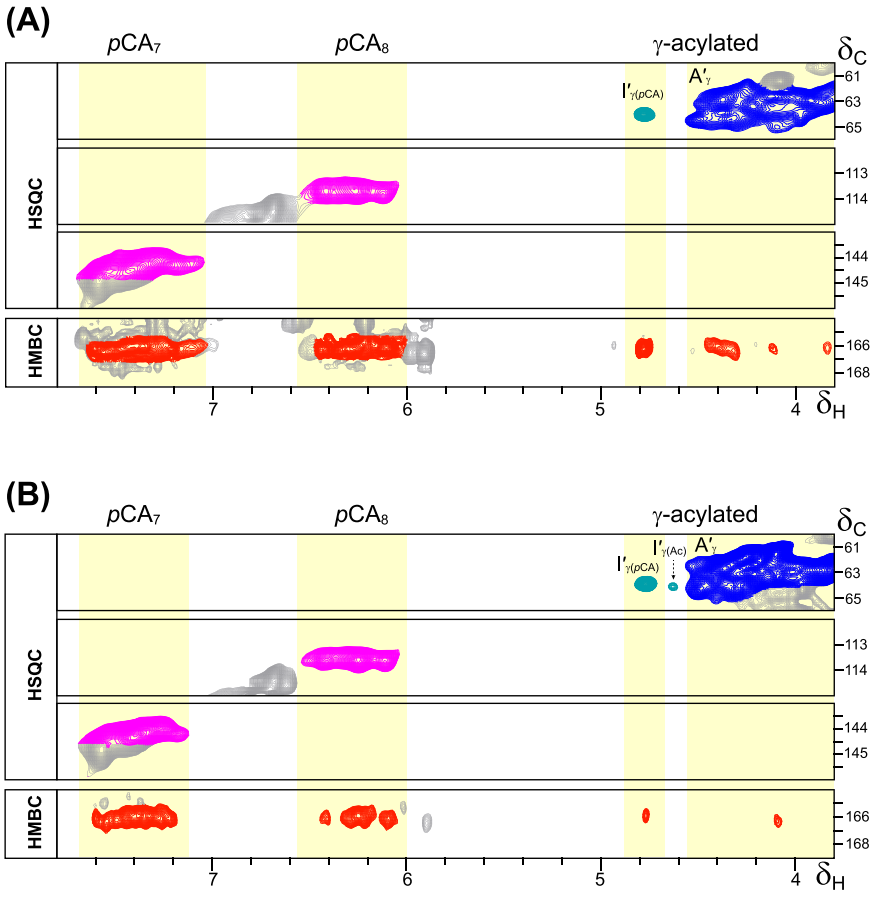

Fig. 5. Sections of the HMBC spectra (δ_C/δ_H 164–169/3.8–7.8) of the MWLs from the rind (A), and the pith (B) of papyrus culms, showing the correlations of the carbonyl carbons of *p*-coumarates (*p*CA) acylating the γ-OH of the lignin. Sections of the HSQC showing the C_γ/H_γ correlations of the γ-acylated lignin (δ_C 60–66) and the C_7/H_7 and C_8/H_8 correlations of *p*-coumarates (δ_C 112–115 and 142–147), are also shown.

γ-acylated tetrahydrofuran structures instead. However, and contrary to what occurs in the lignins of other highly *p*-coumaroylated lignins that present significant amounts of β−β′ tetrahydrofurans (del Río et al., 2012a), these tetrahydrofuran structures were present in relatively low abundances in the papyrus lignins, where they accounted for only 1% and 2% of all linkages in the lignins of the rind and pith, respectively. It has been indicated that the polymerization of lignin begins through the dimerization of monolignols producing resinols (Ralph et al., 2004a, 2004b). In the case of grasses and other monocotyledonous plants with highly acylated lignins, tetrahydrofurans will be the dimerization products formed to start the lignin chain. The low amounts of resinols and tetrahydrofurans that are supposed to initiate polymerization in the papyrus lignins are probably linked to the fact that the lignin chains are initiated also by the flavone tricin present in these lignins, and possible by the other flavonoids too, as already indicated in grasses and other monocots (Lan et al., 2015; del Río et al., 2020, 2021).

3.5. Nature of the groups that acylate the γ-OH of the lignin side-chains

The HSQC spectra of the rind and pith lignins indicated that the γ-OH of the lignin side-chains were highly acylated. However, they did not give much information on the identity of the acylating groups. The presence of important amounts of *p*-coumarates in these lignins, as shown by Py-TMAH and 2D-HSQC NMR, along with the characteristic signal in the spectrum for *p*-hydroxycinnamyl alcohol end-groups acylated with *p*-coumarates $I_{\gamma(pCA)}$, indicates that *p*CA could be the main group that acylates these lignins. To confirm this assumption, the lignins from the rind and pith of papyrus culms were analyzed by 2D-HMBC NMR long-range correlation experiments, as previously used for other highly *p*-coumaroylated lignins (Ralph et al., 1994; del Río et al., 2015). Fig. 5 shows the HMBC sections for the correlations of the carbonyl carbon of *p*-coumarate esters in both lignins. Characteristic signals were observed for the correlations of the carbonyl group of *p*-coumarate esters at δ_C 166.0 with their 7- and 8-protons at $\delta_H \sim 7.40$ and 6.30, as well as with protons around δ_H 4.0–4.8 in the HMBC spectra of both lignins, which were more evident in the lignin of the rind, confirming that *p*-coumarates acylate the γ-OH in these lignins.

Additional information regarding the nature and extent of acylation of the γ-OH in these lignins was obtained by DFRC, a chemical degradative method that selectively cleaves β-ether bonds in lignin, releasing the lignin monomers involved in those linkages (Lu and Ralph, 1997; Regner et al., 2018). A characteristic and distinctive feature of the DFRC method in comparison with other degradative methods is that it leaves γ-esters intact, thus allowing the release of γ-acylated monolignols. Fig. 6 shows the chromatograms of the compounds released upon DFRC of the MWLs from the rind and pith of papyrus culms. The main compounds released were the *cis*- and *trans*-isomers of *p*-hydroxyphenyl (*t*H), guaiacyl (*c*G and *t*G), and syringyl (*c*S and *t*S) lignin monomers arising from the normal (non-acylated) γ-OH lignin units involved in β-ether linkages. A predominance of the G-units was observed in both lignins. In addition, significant amounts of the *cis*- and *trans*-isomers of the sinapyl dihydro-*p*-coumarate (cS_{pCA}, tS_{pCA}) were also released, along with minor amounts of the guaiacyl analogues (cG_{pCA}, tG_{pCA}). Monolignol-ferulate conjugates, which have been shown to be present in the lignins of some plants (Karlen et al., 2016), were not be found, indicating that the ferulates present in these lignins were probably incorporated into the lignin structure by ether linkages or carbon-carbon bonds. The DFRC analyses thus confirmed that *p*-coumarates were the main groups that

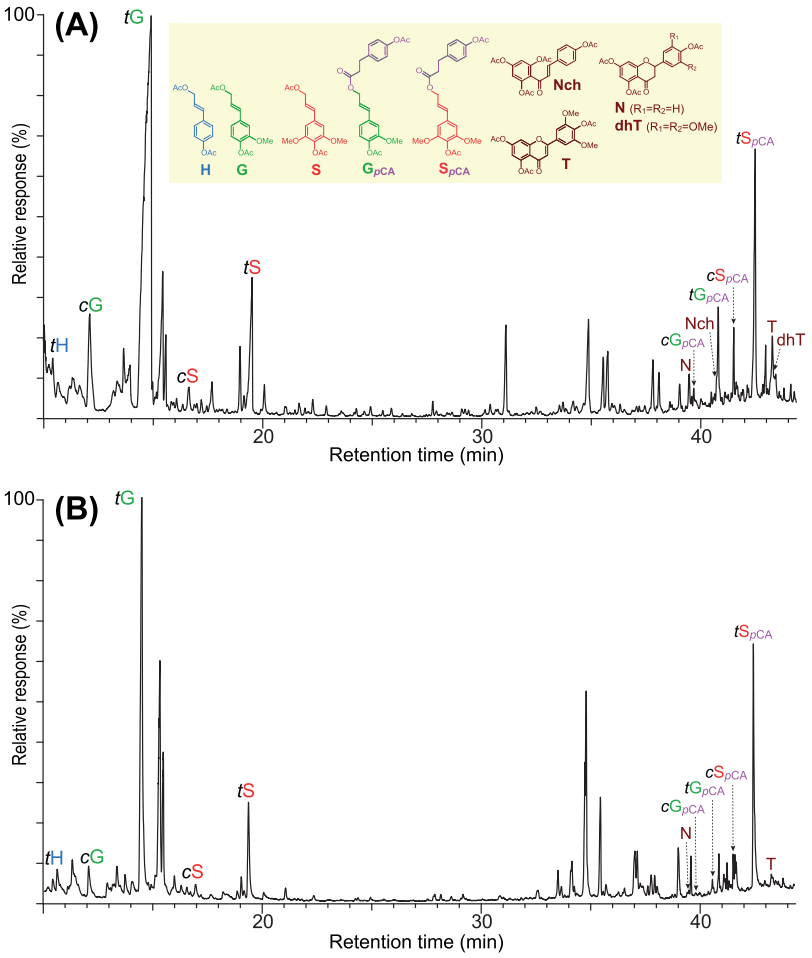

Fig. 6. Chromatograms of the DFRC degradation products released from the MWL preparations from the rind (A) and pith (B) of papyrus culms. *t*H, *c*G, *t*G, *c*S and *t*S are the *cis*- and *trans*-*p*-coumaryl (H), coniferyl (G) and sinapyl (S) alcohol monomers; cG_{pCA}, tG_{pCA}, cS_{pCA}, and tS_{pCA} are the *cis*- and *trans*-coniferyl- and sinapyl-dihydro-*p*-coumarates; Nch: naringenin chalcone; N: naringenin; dhT: dihydrotricin; T: tricin. Note that all compounds are released as their acetate derivatives.

Table 5
Relative molar abundance of the non-acylated γ-OH *p*-hydroxyphenyl (H), guaiacyl (G) and syringyl (S) lignin units, and the γ-acetylated (G_{ac}, S_{ac}), and γ-*p*-coumaroylated (G_{pCA}, S_{pCA}) lignin units, and flavonoids (tricin, T; naringenin, N; dihydrotricin, dhT; naringenin chalcone, Nch), obtained from DFRC and DFRC' degradation of the MWLs from the rind and pith of papyrus culms. The percentages of acetylated and *p*-coumaroylated lignin units are also shown.

	H	G	G_{ac}	G_{pCA}	S	S_{ac}	S_{pCA}	T[a]	N[a]	dhT[a]	Nch[a]	$\%G_{ac}$[b]	$\%G_{pCA}$[b]	$\%S_{ac}$[c]	$\%S_{pCA}$[c]
MWL rind	3.1	76.8	1.6	2.3	8.7	0.3	7.2	3.0	1.2	0.3	0.6	2.0	2.9	1.9	44.4
MWL pith	1.6	62.1	6.3	1.8	11.3	0.6	16.3	0.5	0.2	tr	tr	9.0	2.6	2.1	57.8

H: *p*-hydroxyphenyl units; G: guaiacyl units; S: syringyl units; G_{ac}: acetylated guaiacyl units; S_{ac}: acetylated syringyl units; G_{pCA}: *p*-coumaroylated guaiacyl units; S_{pCA}: *p*-coumaroylated syringyl units; T: tricin; N: naringenin; dhT: dihydrotricin; Nch: naringenin chalcone.
tr: trace amounts
[a] T, N, dhT and Nch molar contents referred to as to the percentage of total lignin units ($H+G+G_{ac}+G_{pCA}+S+S_{ac}+S_{pCA}= 100$).
[b] $\%G_{ac}$ and $\%G_{pCA}$ are the percentages of acetylated (G_{ac}) and *p*-coumaroylated (G_{pCA}) G-units with respect to the total G-units ($G+G_{ac}+G_{pCA}$).
[c] $\%S_{ac}$ and $\%S_{pCA}$ are the percentages of acetylated (S_{ac}) and *p*-coumaroylated (S_{pCA}) S-units with respect to the total S-units ($S+S_{ac}+S_{pCA}$).

acylated the γ-OH in these lignins, and also indicated that *p*-coumaroylation occurred preferentially at S units. Although the mechanism of monolignol *p*-coumaroylation has not been investigated in this particular plant, it is likely that it is similar to that described for grasses which involves *p*-coumaroyl-CoA:monolignol transferases with higher affinity for sinapyl alcohol (Withers et al., 2012; Marita et al., 2014). In addition, the DFRC also released significant amounts of the flavone tricin (T), which was more abundant in the lignin of the rind, in agreement with the NMR data. Tricin is widely present incorporated into the lignin of grasses and other monocotyledonous plants (del Río et al., 2012b, 2015, 2020, 2021; Rencoret et al., 2013; Lan et al., 2015, 2016). Tricin can only form β–*O*–4′ linkages within the lignin polymer, and hence it can be easily released upon DFRC and other chemical degradative methods that cleave β-ether bonds and subsequently analyzed by either LC-MS or GC-MS (Lan et al., 2016; Rosado et al., 2021). Interestingly, other flavonoids could also be identified among the DFRC degradation products, including the flavanones naringenin (N) and dihydrotricin (dhT), as well as the naringenin chalcone (Nch), in agreement with the signals observed in the HSQC spectra. Their identification was achieved by comparison with authentic standards as published elsewhere (Rencoret et al., 2021).

On the other hand, acetates are also known to acylate the γ-OH of lignins in many plants (Ralph, 1996; del Río et al., 2007a, 2008), and the appearance of the characteristic signal of *p*-hydroxycinnamyl acetate

$I_{\gamma(Ac)}$ in the HSQC of the MWL of the pith indicates that acetates also acylate the γ-OH in these lignins. However, the original DFRC degradation protocol uses acetate reagents and therefore cannot be used to investigate the presence of native acetates attached to the γ-OH. But following the same protocol and using propionylating reagents (DFRC') instead of acetylating ones, it is possible to analyze the presence of native acetylated units in the lignins (Ralph and Lu, 1998; del Río et al., 2007b). The DFRC' analysis confirmed that the lignins of the rind and pith of papyrus culms were also acetylated at the γ-OH, although to a lesser degree.

The results of the DFRC (and DFRC') analysis, including the relative abundances of the different lignin monomeric units (H, G, S, G_{ac}, S_{ac}, G_{pCA}, S_{pCA}), the flavonoids (T, N, dhT, Nch), and the percentages of γ-acetylated (%G_{ac}, %S_{ac}) and γ-*p*-coumaroylated (%G_{pCA}, %S_{pCA}) lignin units, are shown in Table 5. The results corroborated that both lignins were highly acylated, and demonstrated that *p*-coumarate was the main group that acylated the γ-OH in these lignins, being predominantly attached to S-lignin units. Hence, in the rind lignin, 44.4% of S-units and 2.9% of G-units were *p*-coumaroylated, while in the pith lignin, 57.8% of S-units and 2.6% of G-units were *p*-coumaroylated. Acetates were also found acylating the γ-OH of these lignins, although to a lesser extent (1.9% of S-units and 2.0% of G-units were acetylated in the rind, while 2.1% of S-units and 9.0% of G-units were acetylated in the pith). Interestingly, while acetylation of the rind lignin showed a slight preference for S-units, similar to *p*-coumaroylation, acetylation of the pith lignin showed a strong preference for G-units. Similar preferences were observed for the lignins of the rind and pith of elephant grass (del Río et al., 2012a). Finally, significant amounts of tricin (3.0%) and naringenin (1.2%), along with lower amounts of dihydrotricin (0.3%) and naringenin chalcone (0.6%) were also released from the rind lignin; in the pith lignin, however, lower amounts of tricin (0.5%), and naringenin (0.2%) could be released whereas only trace amounts of dihydrotricin and naringenin chalcone were found.

4. Conclusions

The lignins of the rind and pith of the papyrus culms were isolated by aqueous dioxane and thoroughly studied by using advanced analytical techniques in lignin characterization. The rind lignin was composed mainly of G-units, with a H:G:S of 4:63:33 (S/G 0.52), whereas the pith lignin had a slightly higher abundance of S-units, with a H:G:S of 8:43:49 (S/G 1.14). The rind lignin had a lower content of β–*O*–4′ alkyl aryl ethers (77% of all measured linkages) than the pith lignin, where they accounted for up to 85% of all linkages. Furthermore, the rind lignin presented a higher abundance of phenylcoumarans (15%), as well as other condensed linkages, than the pith lignin, where they represented only 11% of all measured linkages. Both lignins were highly acylated at the γ-OH with *p*-coumarates, which were mostly attached to S-units. In addition, the rind lignin, and to a lesser extent the pith lignin, contained significant amounts of tricin and other flavonoids (naringenin chalcone, naringenin and dihydrotricin) incorporated into their structure. The data shown in this work provides useful information on the structure of the lignins of the different parts of the papyrus culms, which is of interest to evaluate this material as a source of biomass for the production of biofuels and biomaterials in the context of the lignocellulosic biorefinery.

CRediT authorship Contribution statement

Mario J. Rosado: Investigation, Resources. **Florian Bausch:** Investigation, Resources. **Jorge Rencoret:** Methodology, Investigation. **Gisela Marques:** Methodology, Investigation. **Ana Gutiérrez:** Investigation, Resources; **Thomas Rosenau:** Conceptualization, Investigation, Resources. **Antje Potthast:** Conceptualization, Investigation, Resources. **José C. del Río:** Conceptualization, Investigation, Data Curation, Writing – review & editing.

Declaration of Competing Interest

The authors declare that they have no known competing financial interests or personal relationships that could have appeared to influence the work reported in this paper.

Acknowledgements

This work was partially funded by the Spanish Project AGL2017-83036-R (financed by Agencia Estatal de Investigación, AEI and Fondo Europeo de Desarrollo Regional, FEDER) and by Consejería de Transformación Económica, Industria, Conocimiento y Universidades, Junta de Andalucía, Spain (project P20_00017). MJR thanks the Spanish Ministry of Science, Innovation and Universities for a FPI fellowship (PRE2018-083267). FB, TR, and AP were funded by the Austrian Biorefinery Center Tulln (ABCT). The authors thank Dr. Manuel Angulo for his technical assistance in acquiring the NMR spectra.

References

Abu-Omar, M.M., Barta, K., Beckham, G.T., Luterbacher, J.S., Ralph, J., Rinaldi, R., Román-Leshkov, Y., Samec, J.S.M., Sels, B.F., Wang, F., 2021. Guidelines for performing lignin-first biorefining. Energy Environ. Sci. 14, 262–292. https://doi.org/10.1039/d0ee02870c.

Bajwa, D.S., Pourhashem, G., Ullah, A.H., Bajwa, S.G., 2019. A concise review of current lignin production, applications, products and their environmental impact. Ind. Crops Prod. 139, 111526 https://doi.org/10.1016/j.indcrop.2019.111526.

Björkman, A., 1956. Studies on finely divided wood. Part I. Extraction of lignin with neutral solvents. Sven. Papperstidn. 59, 477–485.

Browning, B.L., 1967. Methods of Wood Chemistry. Wiley-Interscience, New York. https://doi.org/10.1002/pol.1968.160061112.

Chang, C.L., Wang, G.J., Zhang, L.J., Tsai, W.J., Chen, R.Y., Wu, Y.C., Kuo, Y.H., 2010. Cardiovascular protective flavonolignans and flavonoids from *Calamus quiquesetinervius*. Phytochemistry 71, 271–279. https://doi.org/10.1016/j.phytochem.2009.09.025.

Csupor, D., Csorba, A., Hohmann, J., 2016. Recent advances in the analysis of flavonolignans of *Silybum marianum*. J. Pharma. Biomed. Anal. 130, 301–317. https://doi.org/10.1016/j.jpba.2016.05.034.

Darvill, A., McNeil, M., Albersheim, P., Delmer, D., 1980. The primary cell-walls of flowering plants. In: Tolbert, N. (Ed.), The Biochemistry of Plants. Academic Press, New York, pp. 91–162.

del Río, J.C., Martín, F., González-Vila, F.J., 1996. Thermally assisted hydrolysis and alkylation as a novel pyrolytic approach for the structural characterization of natural biopolymers and geomacromolecules. Trends Anal. Chem. 15, 70–79. https://doi.org/10.1016/0165-9936(96)80763-1.

del Río, J.C., Marques, G., Rencoret, J., Martínez, A.T., Gutiérrez, A., 2007a. Occurrence of naturally acetylated lignin units. J. Agric. Food Chem. 55, 5461–5468. https://doi.org/10.1021/jf0705264.

del Río, J.C., Gutiérrez, A., Rodríguez, I.M., Ibarra, D., Martínez, A.,T., 2007b. Composition of non-woody plant lignins and cinnamic acids by Py-GC/MS, Py/TMAH and FT-IR. J. Anal. Appl. Pyrol. 79, 39–46. https://doi.org/10.1016/j.jaap.2006.09.003.

del Río, J.C., Rencoret, J., Marques, G., Gutiérrez, A., Ibarra, D., Santos, J.I., Jiménez-Barbero, J., Zhang, L., Martínez, A.T., 2008. Highly acylated (acetylated and/or *p*-coumaroylated) native lignins from diverse herbaceous plants. J. Agric. Food Chem. 56, 9525–9534. https://doi.org/10.1021/jf800806h.

del Río, J.C., Prinsen, P., Rencoret, J., Nieto, L., Jiménez-Barbero, J., Ralph, J., Martínez, A.T., Gutiérrez, A., 2012a. Structural characterization of the lignin in the cortex and pith of elephant grass (*Pennisetum purpureum*) stems. J. Agric. Food Chem. 60, 3619–3634. https://doi.org/10.1021/jf300099g.

del Río, J.C., Rencoret, J., Prinsen, P., Martínez, A.T., Ralph, J., Gutiérrez, A., 2012b. Structural characterization of wheat straw lignin as revealed by analytical pyrolysis, 2D NMR, and reductive cleavage methods. J. Agric. Food Chem. 60, 5922–5935. https://doi.org/10.1021/jf301002n.

del Río, J.C., Lino, A.G., Colodette, J.L., Lima, C.F., Gutiérrez, A., Martínez, A.T., Lu, F., Ralph, J., Rencoret, J., 2015. Differences in the chemical structures of the lignins from sugarcane bagasse and straw. Biomass Bioenergy 81, 322–338. https://doi.org/10.1016/j.biombioe.2015.07.006.

del Río, J.C., Rencoret, J., Gutiérrez, A., Kim, H., Ralph, J., 2018. Structural characterization of lignin from maize (*Zea mays* L.) fibers: evidences for diferuloylputrescine incorporated into the lignin polymer in maize kernels. J. Agric. Food Chem. 66, 4402–4413. https://doi.org/10.1021/acs.jafc.8b00880.

del Río, J.C., Rencoret, J., Gutiérrez, A., Elder, T., Kim, H., Ralph, J., 2020. Lignin monomers from beyond the canonical monolignol biosynthetic pathway – another brick in the wall. ACS Sustain. Chem. Eng 8, 4997–5012. https://doi.org/10.1021/acssuschemeng.0c01109.

del Río, J.C., Rencoret, J., Gutiérrez, A., Lan, W., Kim, H., Ralph, J., 2021. Lignin monomers derived from the flavonoid and hydroxystilbene biosynthetic pathways. In: Reed, J., de Freitas, V., Quideau, S. (Eds.), Recent Advances in Polyphenol

Research, Volume 7. Wiley-Blackwell, pp. 177–206. https://doi.org/10.1002/9781119545958.ch7.
Hatfield, R.D., Rancour, D.M., Marita, J.M., 2017. Grass cell walls: a story of cross-linking. Front. Plant Sci. 7, 2056. https://doi.org/10.3389/fpls.2016.02056.
Jones, M., Muthuri, F., 1997. Standing biomass and carbon distribution in a papyrus (*Cyperus papyrus* L.) swamp on Lake Naivasha, Kenya. J. Trop. Ecol. 13, 347–356. https://doi.org/10.1017/S0266467400010555.
Jones, M.B., 2011. C_4 species as energy crops. In: Raghavendra, A.S., Sage, R.F. (Eds.), C_4 Photosynthesis and Related CO_2 Concentrating Mechanisms. Springer, Dordrecht, pp. 379–397.
Jones, M.B., Kansiime, F., Suanders, M.J., 2018. The potential use of papyrus (*Cyperus papyrus* L.) wetlands as a source of biomass energy for sub-Saharan Africa. GCB Bioenergy 10, 4–11. https://doi.org/10.1111/gcbb.12392.
Karlen, S.D., Zhang, C., Peck, M.L., Smith, R.A., Padmakshan, D., Helmich, K.E., Free, H. C.A., Lee, S., Smith, B.G., Lu, F., Sedbrook, J.C., Sibout, R., Grabber, J.H., Runge, T. M., Mysore, K.S., Harris, P.J., Bartley, L.E., Ralph, J., 2016. Monolignol ferulate conjugates are naturally incorporated into plant lignins. Sci. Adv. 2, e1600393 https://doi.org/10.1126/sciadv.1600393.
Karlen, S.D., Free, H.C.A., Padmakshan, D., Smith, B.G., Ralph, J., Harris, P.J., 2018. Commelinid monocotyledon lignins are acylated by *p*-coumarate. Plant Physiol. 177, 513–521. https://doi.org/10.1104/pp.18.00298.
Kim, H., Ralph, J., Akiyama, T., 2008. Solution-state 2D NMR of ball-milled plant cell-wall gels in DMSO-d_6. Bioenergy Res. 1, 56–66. https://doi.org/10.1007/s12155-008-9004-z.
Kim, H., Padmakshan, D., Li, Y., Rencoret, J., Hatfield, R., Ralph, J., 2017. Characterization and elimination of undesirable protein residues in plant cell wall materials for enhancing lignin analysis by solution-state nuclear magnetic resonance spectroscopy. Biomacromolecules 18, 4184–4195. https://doi.org/10.1021/acs.biomac.7b01223.
Lan, W., Lu, F., Regner, M., Zhu, Y., Rencoret, J., Ralph, S.A., Zakai, U.I., Morreel, K., Boerjan, W., Ralph, J., 2015. Tricin, a flavonoid monomer in monocot lignification. Plant Physiol. 167, 1284–1295. https://doi.org/10.1104/pp.114.253757.
Lan, W., Rencoret, J., Lu, F., Karlen, S.D., Smith, B.G., Harris, P.J., del Río, J.C., Ralph, J., 2016. Tricin-lignins: occurrence and quantitation of tricin in relation to phylogeny. Plant J. 88, 1046–1057. https://doi.org/10.1111/tpj.13315.
Lu, F., Ralph, J., 1997. Derivatization followed by reductive cleavage (DFRC method), a new method for lignin analysis: Protocol for analysis of DFRC monomers. J. Agric. Food Chem. 45, 2590–2592. https://doi.org/10.1021/jf970258h.
Lu, F., Ralph, J., 2002. Preliminary evidence for sinapyl acetate as a lignin monomer in kenaf. Chem. Commun. 1, 90–91. https://doi.org/10.1039/B109876D.
Lu, F., Ralph, J., 2005. Novel β–β structures in lignins incorporating acylated monolignols. Appita 233–237.
Lu, F., Ralph, J., 2008. Novel tetrahydrofuran structures derived from β–β-coupling reactions involving sinapyl acetates in kenaf lignins. Org. Biomol. Chem. 6, 3681–3694. https://doi.org/10.1039/B809464K.
Lu, F., Karlen, S., Regner, M., Kim, H., Ralph, S., Sun, R.-C., Kuroda, K.-i, Augustin, M., Mawson, R., Sabarez, H., Singh, T., Jimenez-Monteon, G., Zakaria, S., Hill, S., Harris, P., Boerjan, W., Wilkerson, C., Mansfield, S., Ralph, J., 2015. Naturally *p*-hydroxybenzoylated lignins in palms. BioEnergy Res. 8, 934–952. https://doi.org/10.1007/s12155-015-9583-4.
Marita, J.M., Hatfield, R.D., Rancour, D.M., Frost, K.E., 2014. Identification and suppression of the *p*-coumaroyl CoA:hydroxycinnamyl alcohol transferase in *Zea mays* L. Plant J. 78, 850–864. https://doi.org/10.1111/tpj.12510.
Mnaya, B., Asaeda, T., Kiwango, Y., Ayubu, E., 2007. Primary production in papyrus (*Cyperus papyrus* L.) of Rubondo Island, Lake Victoria, Tanzania. Wetl. Ecol. Manag. 15, 269–275. https://doi.org/10.1007/s11273-006-9027-1.
Muthuri, F.M., Jones, M.B., Imbamba, S.K., 1989. Primary productivity of papyrus (*Cyperus papyrus* L.) in a tropical swamp: Lake Naivasha. Kenya Biomass 18, 1–14. https://doi.org/10.1016/0144-4565(89)90077-2.
Nguyen, L.T., Phan, D.P., Sarwar, A., Tran, M.H., Lee, O.K., Lee, E.Y., 2021. Valorization of industrial lignin to value-added chemicals by chemical depolymerization and biological conversion. Ind. Crops Prod. 161, 113219 https://doi.org/10.1016/j.indcrop.2020.113219.
Nicholson, P.T., Shaw, I., 2000. Ancient Egyptian Materials and Technology. Cambridge University Press, Cambridge, UK.
Pikovskoi, I.I., Kosyakov, D.S., Faleva, A.V., Shavrina, I.S., Kozhevnikov, A., Yu, Ulʹyanovskii, N.V., 2020. Study of the sedge (*Cárex*) lignin by high-resolution mass spectrometry and NMR spectroscopy. Russian Chem. Bull. Int. Ed. 69, 2004–2012. https://doi.org/10.1007/s11172-020-2992-3.
Ralph, J., Hatfield, R.D., 1991. Pyrolysis-GC-MS characterization of forage materials. J. Agric. Food Chem. 39, 1426–1437. https://doi.org/10.1021/jf00008a014.
Ralph, J., Hatfield, R.D., Quideau, S., Helm, R.F., Grabber, J.H., Jung, H.-J.G., 1994. Pathway of *p*-coumaric acid incorporation into maize lignin as revealed by NMR. J. Am. Chem. Soc. 116, 9448–9456. https://doi.org/10.1021/ja00100a006.
Ralph, J., 1996. An unusual lignin from kenaf. J. Nat. Prod. 59, 341–342. https://doi.org/10.1021/np960143s.
Ralph, J., Lu, F., 1998. The DRC method for lignin analysis. 6. A simple modification for identifying natural acetates in lignin. J. Agric. Food Chem. 46, 4616–4619. https://doi.org/10.1021/jf980680d.
Ralph, J., Lundquist, K., Brunow, G., Lu, F., Kim, H., Schatz, P.F., Marita, J.M., Hatfield, R.D., Ralph, S.A., Christensen, J.H., Boerjan, W., 2004a. Lignins: natural polymers from oxidative coupling of 4-hydroxyphenylpropanoids. Phytochem. Rev. 3, 29–60. https://doi.org/10.1023/b:phyt.0000047809.65444.a4.
Ralph, S.A., Ralph, J., Landucci, L., 2004b. NMR Database of Lignin and Cell Wall Model Compounds. US Forest Prod. Lab., Madison, WI (⟨http://ars.usda.gov/Services/docs.htm?docid=10491⟩) (accessed: April 2020).
Ralph, J., 2010. Hydroxycinnamates in lignification. Phytochem. Rev. 9, 65–83. https://doi.org/10.1007/s11101-009-9141-9.
Regner, M., Bartuce, A., Padmakshan, D., Ralph, J., Karlen, S.D., 2018. Reductive cleavage method for quantitation of monolignols and low-abundance monolignol conjugates. ChemSusChem 11, 1580–1605. https://doi.org/10.1002/cssc.201800958.
Rencoret, J., Marques, G., Gutiérrez, A., Nieto, L., Santos, J.I., Jiménez-Barbero, J., Martínez, A.T., del Río, J.C., 2009. HSQC NMR analysis of lignin in woody (*Eucalyptus globulus* and *Picea abies*) and non-woody (*Agave sisalana*) ball-milled plant materials at the gel state. Holzforschung 63, 691–698. https://doi.org/10.1515/HF.2009.070.
Rencoret, J., Ralph, J., Marques, G., Gutiérrez, A., Martínez, A.T., del Río, J.C., 2013. Structural characterization of lignin isolated from coconut (*Cocos nucifera*) coir fibers. J. Agric. Food Chem. 61, 2434–2445. https://doi.org/10.1021/jf304686x.
Rencoret, J., Prinsen, P., Gutiérrez, A., Martínez, A.T., del Río, J.C., 2015. Isolation and structural characterization of the milled wood lignin, dioxane lignin, and cellulolytic lignin preparations from brewerś spent grain. J. Agric. Food Chem. 63, 603–613. https://doi.org/10.1021/jf505808c.
Rencoret, J., Kim, H., Evaristo, A.B., Gutiérrez, A., Ralph, J., del Río, J.C., 2018. Variability in lignin composition and structure in cell walls of different parts of macaúba (*Acrocomia aculeata*) palm fruit. J. Agric. Food Chem. 66, 138–153. https://doi.org/10.1021/acs.jafc.7b04638.
Rencoret, J., Rosado, M.J., Kim, H., Tymokhin, V., Gutiérrez, A., Bausch, F., Rosenau, T., Potthast, A., Ralph, J., del Río, J.C., 2021. Flavonoids naringenin chalcone, naringenin, dihydrotricin, and tricin are lignin monomers in papyrus. Plant Physiol. https://doi.org/10.1093/plphys/kiab469.
Rinaldi, R., Jastrzebshi, R., Clough, M.T., Ralph, J., Kennema, M., Bruijnincx, P.C.A., Weckhuysen, B.M., 2016. Paving the way for lignin valorisation: recent advances in bioengineering, biorefining and catalysis. Angew. Chem. Int. Ed. 55, 8164–8215.
Rosado, M.J., Rencoret, J., Marques, G., Gutiérrez, A., del Río, J.C., 2021. Structural characteristics of the guaiacyl-rich lignins from rice (*Oryza sativa* L.) husks and straw. Front. Plant Sci. 12, 640475 https://doi.org/10.3389/fpls.2021.640475.
Tappi, 2004. Tappi Test Methods 2004-2005. Tappi Press, Norcoss, GA, USA.
Tolbert, A., Akinosho, H., Khunsupat, R., Naskar, A.K., Ragauskas, A.J., 2014. Characterization and analysis of the molecular weight of lignin for biorefining studies. Biofuel. Bioprod. Biorefin. 8, 836–856. https://doi.org/10.1002/bbb.1500.
Withers, S., Lu, F., Kim, H., Zhu, Y., Ralph, J., Wilkerson, C.G., 2012. Identification of a grass-specific enzyme that acylates monolignols with *p*-coumarate. J. Biol. Chem. 287, 8347–8355. https://doi.org/10.1074/jbc.M111.284497.
Yuan, M., Ao, Y., Yao, N., Xie, J., Zhang, D., Zhang, J., Zhang, X., Ye, W., 2019. Two new flavonoids from the nuts of *Areca catechu*. Molecules 24, 2862. https://doi.org/10.3390/molecules24162862.